Int. J. Metrol. Qual. Eng. **14**, 13 (2023)

https://doi.org/10.1051/ijmqe/2023011

International Journal of Metrology and Quality Engineering

Available online at:
www.metrology-journal.org

RESEARCH ARTICLE

OPEN ACCESS

Acoustic thermometer operating up to 11 m: uncertainty assessment and new values for Cramer coefficients around 40 kHz

Karim Mimoune, Joffray Guillory*, and Mark Plimmer

Received: 29 November 2022 / Accepted: 17 July 2023

Abstract. The present article describes an acoustic thermometer to measure the average air temperature integrated along a path ranging from 1 m to 11 m. It is based on time-of-flight measurement of ultrasound pulses at frequencies close to 40 kHz. Several methods for the detection of arrival times were investigated, notably cross-correlation and cross-spectrum. The uncertainty of the instrument itself, independent of that of the Cramer equation has been estimated at between 0.13 K to 0.09 K for distances ranging from 3 m to 11 m respectively. In practice, an experimental comparison with Pt100 probes (uncertainty of 0.1 K) has shown that the estimated uncertainty levels are relatively compatible, although the linearity of the system does not appear to be very good. To solve this problem, appropriate values for the Cramer coefficients a_0 and a_1 for an acoustic frequency of about 40 kHz have been determined, which contributes to improved knowledge of this equation as a function of acoustic frequency.

1 Introduction

The measurement of distances in air by optical means, notably laser telemetry, requires an accurate knowledge of the refractive index n of the medium. To measure a distance of 10 m with an accuracy of 10 µm, we need to know n to within 1 part in 10^6 (1 ppm). At a given wavelength, n is a function of the thermodynamic temperature T, the atmospheric pressure p and, to a lesser extent, the partial pressure of water vapour p_w (often expressed by the humidity sensors as RH, i.e., a percentage of the saturated water vapour pressure), and the carbon dioxide concentration (CO_2) x_c. The influence of these parameters (Tab. 1) has been studied for decades in the way of the pioneering work of Edlén [1], and it has become usual to measure T, p, RH and x_c to calculate n using an updated version of the Edlén's semi-empirical equation, e.g., that of Bönsch and Potulski [2] which was tested at the 10^{-8} level. It is thus the measurement of the atmospheric parameters that dominates the uncertainty in n.

To broaden the subject slightly, when distance measurements in air are achieved by microwaves of several GHz, it turns that variation of partial pressure of water vapour rather than temperature is the limiting factor: microwaves are more sensitive than optics to humidity by a factor of 20 [3].

While atmospheric presssure and CO_2 concentration are largely isotropic[1] and slowly varying on the timescale of a distance measurement, rapidly varying temperature in time (over a few seconds) and space (e.g., vertical gradients of 1 K/m [4]) are potentially large sources of systematic error[2]. The temperature along an optical path must therefore be determined in real time.

Several methods exist to measure such a temperature. We can use platinum resistances, but their response time is several seconds. Thermistances have sub-second responses, but are non-linear and require frequent re-calibration. More generally, the use of several thermometers placed at regular intervals along the path soon becomes impractical. Moreover, these contact sensors are poorly suited to the determination of air temperature due to poor thermal contact with the air constituents, self-heating, and the effects of radiation [5], such as solar heating outdoors. To avoid these problems, spectroscopic and acoustic measurements are of great interest.

Laser spectroscopic techniques based on the relative absorption of a pair of lines of atmospheric constituents can be used for distances up to several hundred metres. Using laser diodes to probe molecular oxygen over for a path length

[1] Atmospheric pressure falls with altitude but can be considered constant for a given beam height. At sea level 0.14 hPa/m.

[2] For a constant partial pressure of water vapour, RH is temperature-dependent, but its impact on the refractive index is far less than that of the temperature variation itself.

* Corresponding author: joffray.guillory@cnam.fr

Table 1. Relative sensitivity of optical distance measurements to the variation of environmental parameters around $T = 293$ K, $p = 1013.25$ hPa, $RH = 50\%$ and $x_c = 450$ ppm for an optical wavelength of 1550 nm. Values calculated using the equation of Bönsch and Potulski [2].

Parameter	Contribution
ΔT	−0.95 (µm/m)/K
Δp	+0.27 (µm/m)/hPa
Δp_w	−0.09 µm/m for +10%
Δx_c	+0.03 µm/m for +200 ppm

of 67 m, Hietema and Merimaa [6] obtained an RMS noise of 22 mK. The accuracy of the method relies on the data available for the transition strengths of the lines employed.

Another possibility is acoustic thermometry. NPL has developed such a thermometer [7,8] that measures the air temperature along a fixed path of about 50 cm using an acoustic interferometer. The acoustic frequency, from 10 kHz to 20 kHz, is continuously adjusted to maintain a constant number of wavelengths along the interferometric path. Thus, the speed of sound in air is proportional to the frequency. This instrument was tested in a climate-controlled chamber for temperatures between 230 K and 311 K: comparison with 100 Ω platinum resistance thermometers (Pt100) showed temperature differences of less than 1 K. The uncertainty after calibration of the system was estimated to be 0.1 K.

To determine the air temperature over longer and variable distances, instruments capable of integrating measurements along a path have been developed. MIKES has developed such an acoustic thermometer [9] operating up to 12 m. It measures the propagation time of acoustic pulses of 60 µs duration emitted by piezoelectric transducers. To this end, the phase of the first two pulses detected from the detector is measured using a fast Fourier transform cross-correlation algorithm. The system performs two successive speed-of-sound measurements along two parallel paths, symmetrically disposed with respect to a laser beam, but in opposite directions to compensate for the effect of airflow. Series of measurements between 4.7 m and 5.7 m, for temperatures ranging from 292 K to 295 K, showed an uncertainty of 25 mK once they had redetermined the equation of the speed of sound, i.e., values of the Cramer coefficients appropriate to the working frequency of 50 kHz.

INRiM has also developed acoustic thermometers, one for indoor measurements, the other for long-distance measurements outside [10]. Both are based on the phase difference between two continuous-wave signals propagated in air, an acoustic measurement signal and an optical reference signal (intensity modulation of a laser). The first system was tested along a 28-m-long interferometric bench equipped with 14 calibrated thermistors. The comparison of their acoustic thermometer operating at 20 kHz with the average value of the thermistors showed differences of less than 0.1 K for a temperature around 294.7 K modulated with periodic variations of amplitude 0.3 K. This instrument was also tested outdoors over 78 m. Comparison with three Pt100 thermometers over two hours showed differences of less than 1 K. Finally, the acoustic thermometer dedicated to long-distance measurements was tested over 182 m. To reduce sound attenuation over such a distance, and thus maintain a good signal-to-noise ratio, it used a much lower acoustic frequency, namely 47 Hz. The comparison with eight thermistors distributed along the path showed differences of less than 2 K. The performance was limited by the low spatial sampling of the thermistors and the effect of the wind.

The most recent results from INRiM are presented in [11]. Their acoustic thermometer dedicated to indoor measurement was compared to four calibrated Pt100 sensors in a semi-anechoic chamber. Measurements over 8.2 m, over 9 h for forced temperature changes between 288 K and 293 K, then over three days with natural periodic day-night temperature changes between 285 K and 291 K, demonstrated an uncertainty of 0.1 K for their acoustic thermometer. Similar measurements over 11 m in the temperature range of 279 K – 289 K confirmed this performance.

In summary, 0.1 K is a typical uncertainty for indoor temperature measurements up to 11 m. To obtain smaller uncertainties, as in [9], it becomes necessary to redefine parameters for the speed of sound for the acoustic frequency at which the thermometer is working. For longer distances, acoustic thermometers are more complex to characterise, but comparisons to date have shown differences of less than 2 K for distances up to 182 m.

The remainder of the article is structured as follows. In Section 2, we recall the calculation of the speed of sound, which is measured by our acoustic thermometer in order to deduce the air temperature. Then, we describe the apparatus and experimental method, including the choice of acoustic frequency, pulse characteristics, and methods for the detection of arrival times. The calibration process of the acoustic thermometer is also presented. The results, notably appropriate values for the Cramer coefficients a_0 and a_1 for acoustic frequencies around 40 kHz, are presented in Section 3. It is complementary to the work of Korpelainen and Lassila (from MIKES) who performed a similar determination at 50 kHz. This paper thus contributes to improved knowledge of Cramer coefficients as a function of acoustic frequency. A conclusion is given in Section 4.

2 Apparatus and method

2.1 The speed of sound in air

For an ideal gas, the speed of sound is proportional to the square-root of the thermodynamic temperature. It also depends on the mean molecular mass M, on the ideal gas constant $R = 8.314\,462\,618$ J.K^{-1} mol^{-1} [12], and on the ratio of specific heats $\gamma = C_p/C_v$ at constant pressure and constant volume, whatever the gas pressure p:

$$v = \sqrt{\frac{\gamma RT}{M}}. \tag{1}$$

For a real gas, the speed of sound propagation is given by:

$$v = \sqrt{\frac{\gamma(T)RT}{M}\left(1 + \frac{2pB}{RT}\right)} \tag{2}$$

where B is the second virial coefficient of state. Korpelainen and Lassila [9] stated that the values of B for moist air were not known[3]. Thus, they relied like other workers on more accurate albeit, semi-empirical equations for the zero-frequency speed of sound due to Cramer [16] and Wong [17,18].

Cramer's version, in which the speed of sound in metres per second is given by the sum of 16 terms, is as follows:

$$\begin{aligned} v(\theta, p, x_w, x_c) &= a_0 + a_1\theta + a_2\theta^2 + \left(a_3 + a_4\theta + a_5\theta^2\right)x_w \\ &+ \left(a_6 + a_7\theta + a_8\theta^2\right)p + \left(a_9 + a_{10}\theta + a_{11}\theta^2\right)x_c \\ &+ a_{12}x_w^2 + a_{13}p^2 + a_{14}x_c^2 + a_{15}x_w p x_c \end{aligned} \tag{3}$$

where θ is the temperature in degrees Celsius, p the atmospheric pressure in pascals, and x_w and x_c are the mole fractions of water vapour and carbon dioxide.

To quantify sound wave propagation at non-zero frequencies, the effect of collisions between oxygen and nitrogen molecules, which modify the specific heat ratio, needs to be taken into account. Using the Kramers–Kronig dispersion relationship between ultrasonic attenuation and phase velocity [19], Morfey and Howell [20] proposed a correction of the form:

$$\frac{1}{v_0} - \frac{1}{v_\varphi} = \frac{\alpha_{\nu\mathrm{N}}}{2\pi f_{r\mathrm{N}}} + \frac{\alpha_{\nu\mathrm{O}}}{2\pi f_{r\mathrm{O}}} \tag{4}$$

where v_ϕ is the speed of sound including effects of dispersion, α_{vN} and α_{vo} the plane-wave attenuation coefficients due to vibrational relaxation of N_2 and O_2, respectively, and f_{rN} and f_{ro} the relaxation frequencies for the same molecules. The parameter v_o is the speed of sound at zero frequency given by formula (3).

However, even when this correction is applied, at ultrasonic frequencies, the coefficients of the original Cramer equation do not predict measured sound velocities to within experimental accuracy. The uncertainty in the speed of sound derived from the Cramer equation, estimated to be 300 ppm by Korpelainen and Lassila, was increased to 545 ppm by Wong [18]. This motivated Korpelainen and Lassila to determine more appropriate values of the coefficients a_0 and a_1. Around the time of their work, Zuckerwar [21] published another equation for the speed of sound in air, the estimated accuracy of which is about 1000 ppm. Most recently, Gavioso and colleagues [22] have revisited the work of Zuckerwar and, by including state-of-the art calculations of virial coefficients, e.g. [15], have produced a model with estimated uncertainties at least five times smaller. In the work described in the present paper, where different frequencies were employed (from 38 kHz to 42 kHz), a determination of the coefficients a_0 and a_1 specific to this range proved necessary.

2.2 Principle

The acoustic thermometer is based on the measurement of the time of flight t_{TOF} of acoustic waves travelling in the air over a known distance d. The measured speed of sound v_m is calculated as follows:

$$v_m = \frac{d}{t_{TOF}}. \tag{5}$$

To counteract the effect of air movement, acoustic measurements are performed for ultrasonic waves in opposite directions along parallel paths, yielding two times of flight t_{TOF1} and t_{TOF2}. The average time of flight t_{TOF} is then used to deduce the air temperature integrated along the acoustic path:

$$t_{TOF} = \frac{t_{TOF1} + t_{TOF2}}{2}. \tag{6}$$

A schematic of the apparatus is shown in Figure 1, with a first acoustic path from the transmitter Tx 1 to the receiver Rx 1, and a second one from the transmitter Tx 2 to the receiver Rx 2. The part of the acoustic system that includes the transducers Tx 2 and Rx 1 is called part A. It includes an absolute distance meter (ADM) to determine the distance d between the two parts of the system.

To determine the time of flight of the acoustic waves, we measure the difference of times of arrival (DTOA) between two electrical signals, a reference signal and a measurement one. To this end, a digital signal of the acoustic wave to be transmitted is first built numerically using Matlab software and sent either by Wi-Fi or an Ethernet cable to the signal generators (RedPitaya boards, STEMlab 125-14) of parts A and B.

Next, for each acoustic path, the generated electrical signal modulates the intensity of a distributed feedback laser diode at 1550 nm (Koheron LD101) by driving its current. This laser ensures two things: it generates the reference signal for the DTOA measurement thanks to an internal monitor photodetector, and it transmits the acoustic wave to the distant acoustic transmitter. Indeed, after collimation of the optical beam with a multi-element lens system (Thorlabs F810FC-1550) and propagation in air up to the acoustic transmission part of the system, the signal is received by an amplified photodiode (Thorlabs PDA36A-EC), boosted by an electrical amplifier, and sent to the acoustic transmitter (Cebek C7210). At this stage, the signal is propagated acoustically in the air between the two transducers. After reception by the acoustic receiver (Massa TR-89B), the signal is amplified to be used as the measurement signal for the DTOA measurement. The gain of the electronic amplifiers, designed in-house, can be remotely controlled and is adjusted to avoid saturation of

[3] One supposes they meant no reliable values were available for room temperature. See Lovell-Smith [13] for a discussion of this point. A subsequent calculation by Harvey and Huang [14] gives $B = -29.6$ cm^2/mol with an expanded uncertainty of 4.2 cm^2/mol. The most recent calculations of which we are aware are those due to Garbergoglio et al. [15].

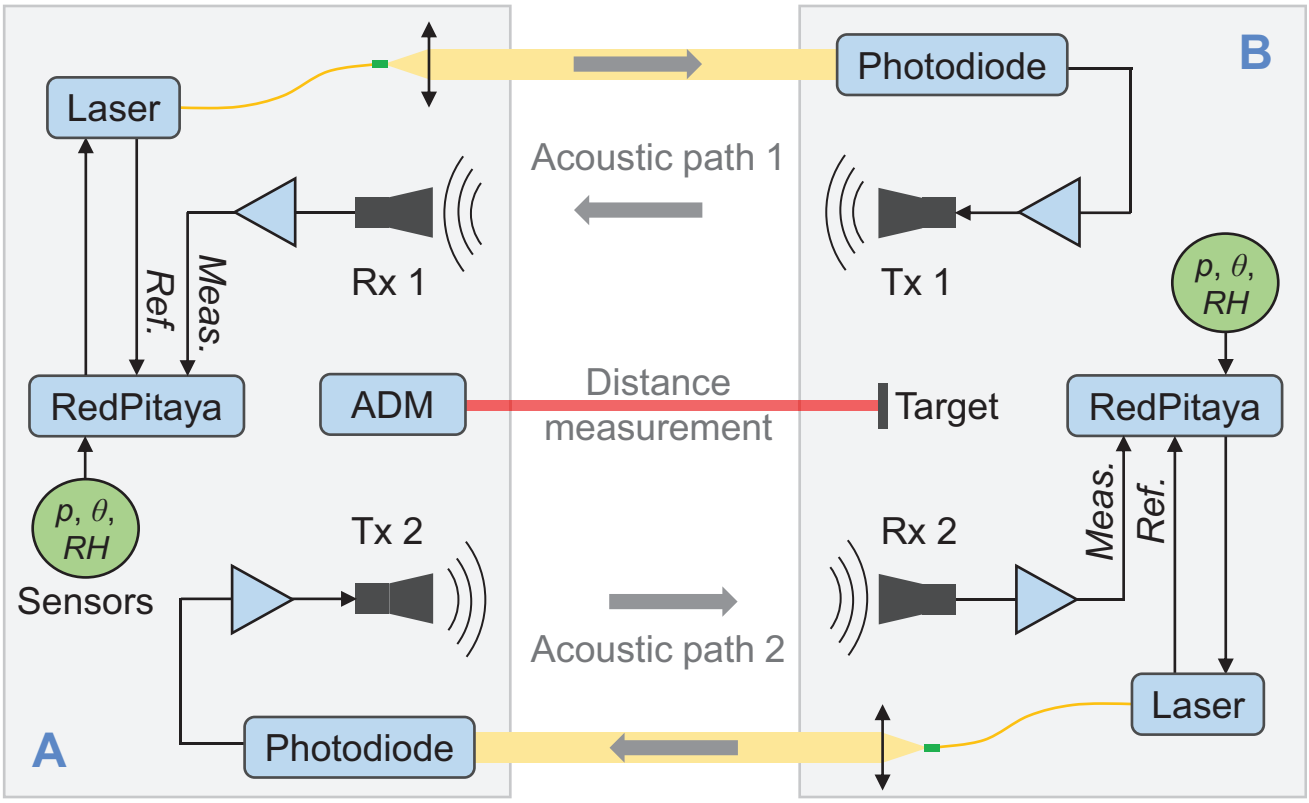

Fig. 1. Principle of the acoustic thermometer

the received signals, while optimizing the transmission and thus increasing the operating distance. These amplifiers were designed to be effective at the working frequencies of the acoustic transducers, namely 38 kHz to 42 kHz.

The reference and measurement signals are captured by acquisition boards (the aforementioned RedPitaya boards) and sent to the computer for signal processing using Matlab software. In the acoustic thermometer, each acoustic path can be used independently. To prevent crosstalk, the measurements on both paths are not performed simultaneously, but rather within an interval of 2.0 s, during which time the airflow is assumed to remain constant. While the time of flight is less than 0.1 s, the interval of over 2.0 s stems from the time required for data processing.

In parallel, the distance d required for speed of sound calculation is measured by a commercial ADM (Leica Disto d210). Ultimately, the ADM developed in-house, part of the multilateration system presented in [23] and of uncertainty of 2.5 µm (k=1), will be used for this distance measurement. Moreover, local sensors measure the atmospheric parameters of the Cramer equation (Bosch BME280 for θ, p and RH and Voltcraft CO-60 for CO_2 content).

User comfort requires inaudible acoustic frequencies, i.e. above 20 kHz, but acoustic attenuation rises with frequency. Thus, piezoelectric transducers operating at low ultrasonic frequencies, around 40 kHz, were selected. The sound attenuation in air at such frequencies, is about 1.3 dB/m. The transducers used are compact, widely available on the market, and offer good directivity. However, to increase the power transmitted to the receivers, horn antennas were used for the acoustic emission as shown in Figure 2.

The system displays a bandwidth of about 3.7 kHz around 40 kHz, with frequencies at which the signal is attenuated by 3 dB of 38.3 kHz and 42.0 kHz.

The system was developed with low cost in mind. The use of inexpensive transducers and electronic components can reduce the signal-to-noise ratio of the received signal compared with when more expensive equipment is employed. Under these hardware constraints, we have sought to optimize the acoustic signal as well as the signal processing techniques to reduce measurement uncertainties and maximize the operating distance. Moreover, the spectral content of the generated signal still had to remain within the bandwidth of the system. These points are addressed in the next section.

2.3 Acoustic signals and signal processing

The signal adopted is an acoustic pulse of 500 µs duration with a rectangular envelope and a linear frequency modulation (chirp) from 38 kHz to 42 kHz. In order to record the reference signal and the measurement one in the same capture, the RedPitaya boards generate an acoustic pulse every 8.389 ms as shown in Figure 3. The corresponding pulse repetition rate is thus 119.2 Hz.

In practice, for distances greater than 2.8 m, there is an ambiguity in the difference of times of arrival (DTOA). The number of cycles, an integer noted n_{cycle} and corresponding to the number of periods of 8.839 ms within

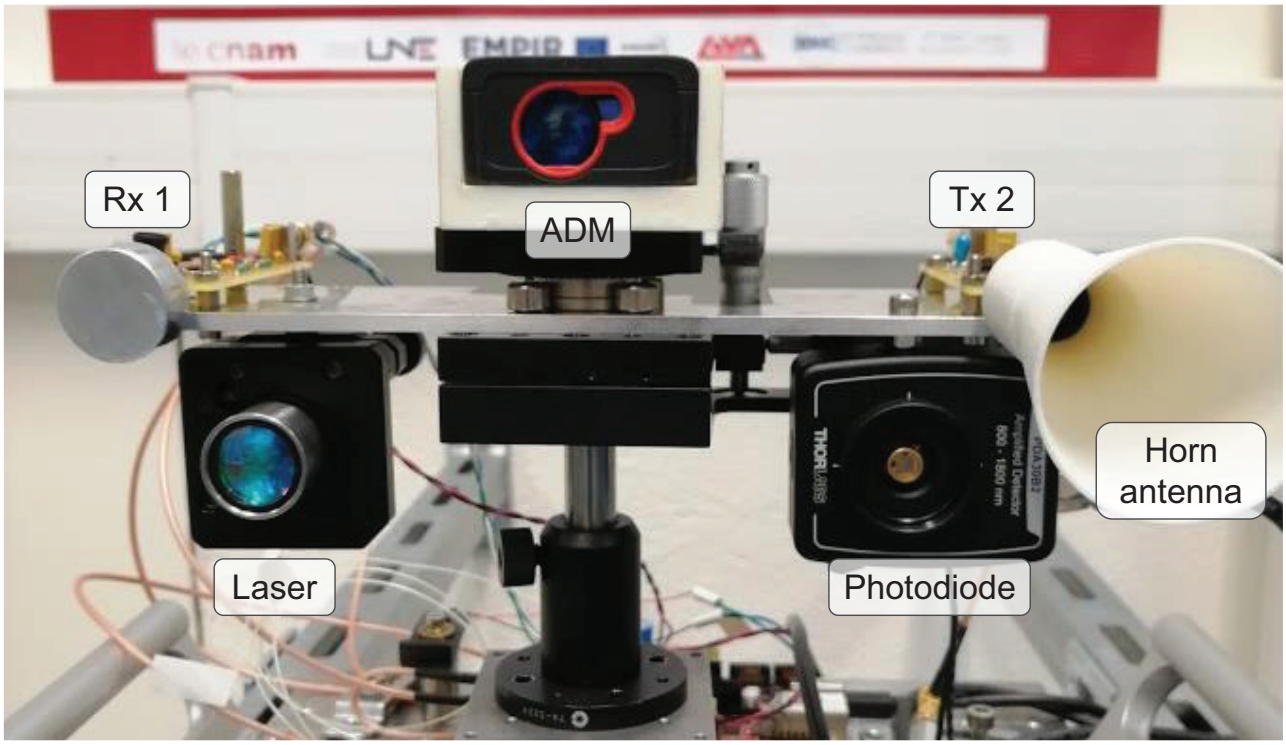

Fig. 2. Photograph of part A of the acoustic thermometer comprising the transmitter Tx 2, the receiver Rx 1, the laser and the absolute distance meter ADM.

the DTOA, has to be determined. From the local environmental sensors, an approximate value of the speed of sound is calculated, after which, from the measured distance d, the expected value of DTOA, and so the number of cycles n_{cycle}, is estimated:

$$t_{DTOA} = t_{measure} + n_{cycle} \times 8.839\,\text{ms}. \tag{7}$$

For reasons of low SNR on the received signals in our measurement conditions, threshold detection techniques were not considered. Techniques such as cross-correlation and its Fourier-domain counterpart, cross-spectrum, provide more efficient noise reduction and were therefore chosen to determine the DTOA between the reference and measurement signals.

A first characterisation of the acoustic thermometer using these techniques was performed with the two parts of the acoustic thermometer separated by 8.471 m. The room temperature, regulated around 296 K, was continuously measured by platinum resistance thermometers (Pt100). Thus, the time of flight for $d = 8.471$ m estimated this way was compared with the DTOA measurement.

The results of a series of 30 successive measurements are shown in Figure 4. For the same signal transmitted, propagated and received by our acoustic thermometer, we can apply two different signal processing method to determine the DTOA, cross-correlation and cross-spectrum. For the upper curves in Figure 4, the room temperature measured by the Pt100 sensors is therefore identical for both methods. This means the reported standard deviations evaluate only the uncertainty due to the method, since the experimental conditions are identical.

The standard deviations of the differences are 1.5 µs with cross-correlation and 2.5 µs with cross-spectrum. These values correspond to the repeatability of the acoustic thermometer, i.e. the standard deviations of measurements made over a short period of time, at a fixed temperature, for the same distance, with the same system, under identical operating conditions.

The method based on cross-correlation exhibits a better repeatability than the one based on cross-spectrum. However, random outliers with deviations of the order of 25 µs sometimes appear, as shown in a second example in Figure 5. These deviations correspond to the period of the acoustic signals which is about 40 kHz. In the end, cross-correlation was adopted as the preferred technique, cross-spectrum, with no outliers, being used merely to correct any errors of the cross-correlation technique whenever they appeared.

Cross-correlation and cross-spectrum are Fourier transform pairs, and therefore in theory provide the same information. In cross-spectrum, the phase shift φ between the transmitted and received signal as a function of frequency f (from 38 kHz to 40 kHz in our case) is a straight line, and a simple linear fit (least-squares minimization) gives the value of $\Delta\phi/\Delta f$ proportional to the DTOA [24]. Thus, by definition, the cross-spectrum technique filters noises outside the acoustic frequencies and can thus be less sensitive to the pulse signal distortions caused by the mechanical inertia of piezoelectric transducers. Indeed, for

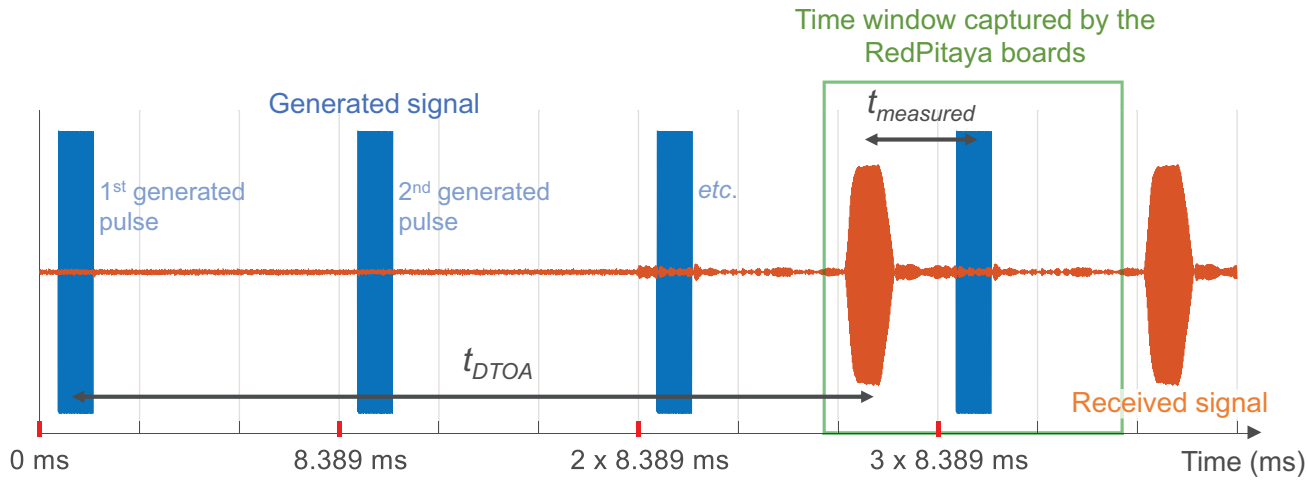

Fig. 3. Illustration of the signals generated every 8.389 ms (in blue), the ones received after acoustic propagation (in orange), and the ones acquired by the RedPitaya boards (in the green box).

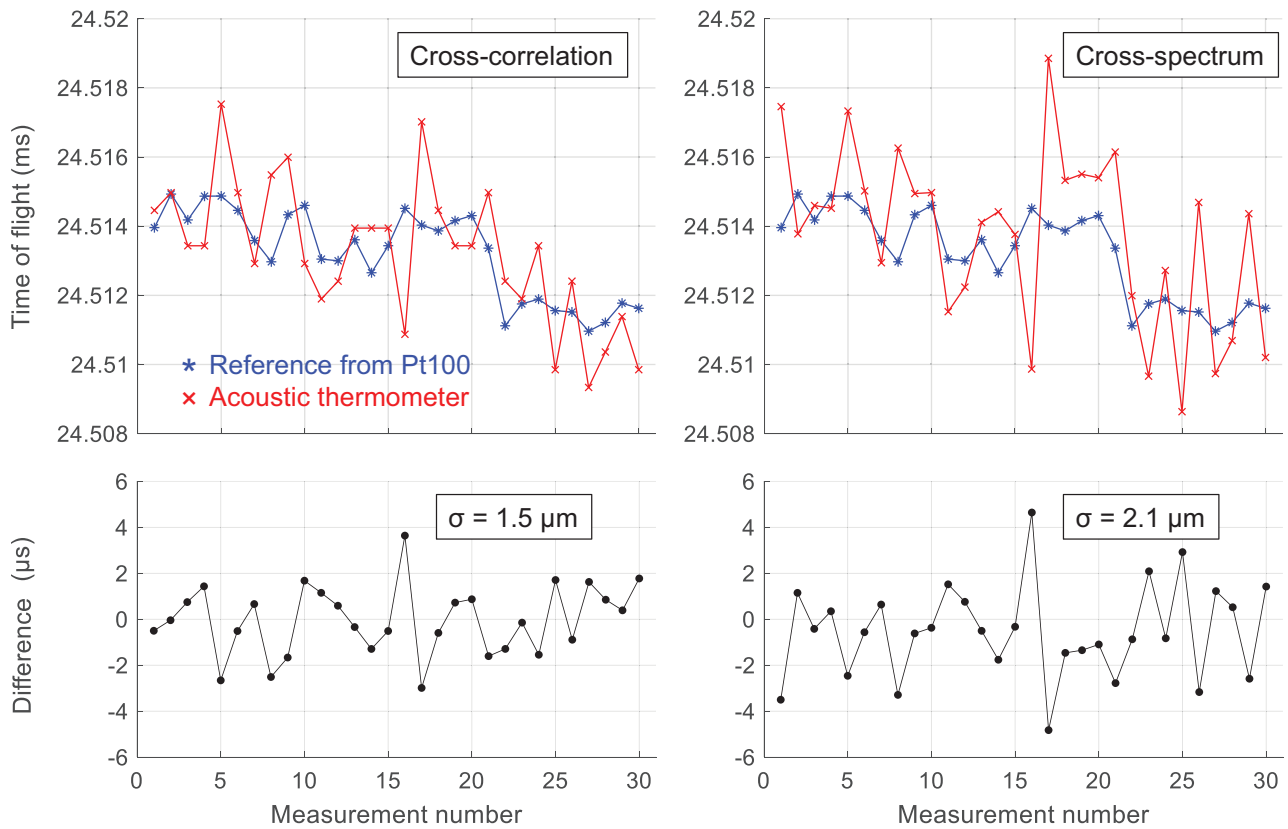

Fig. 4. Above: red crosses the DTOA measured by cross-correlation (on the left) and cross-spectrum (on the right), blue asterisks the values, estimated from the Pt100 probes. Below: the differences between the measurements and the estimations (•). An offset was added to the DTOA values to best fit the time-of-flight values of the measured temperatures.

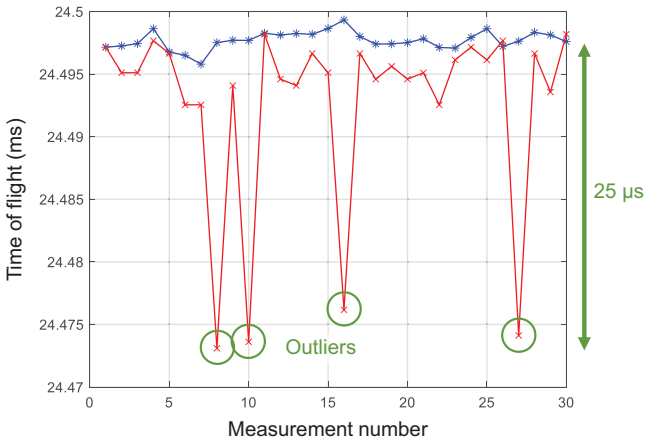

Fig. 5. An example of outliers that occur when cross-correlation is used. Red crosses: DTOA measured by cross-correlation. Blue asterisks: temperature measured by a set of platinum resistance thermometers.

cross-correlation, the whole raw signal is considered. This probably explains why cross-spectrum is more robust and has no outliers in its results. This might also explain the observed difference in standard deviation between the two techniques.

2.4 Calibration process

2.4.1 Time calibration

The time measured by the acoustic thermometer is a difference of times of arrival (DTOA). It includes not only the time of flight (TOF) of the acoustic wave, but also the propagation delay of the signals through the wires, the electronic amplifiers, optical components, etc. This time corresponds to the offset of the instrument t_{offset}:

$$t_{\mathrm{DTOA}} = t_{TOF} + t_{offset}. \tag{8}$$

To perform absolute temperature measurements, the value of this offset needs to be determined; in other words, the system must be calibrated. For this purpose, the system developed was deployed in a 13-metre-long room with air conditioning and the measured temperature compared with a reference air temperature provided by six class B, Pt100 sensors placed along the central axis of the instrument, roughly 30 cm above it. The probes were deployed in a straight line along the length of the laboratory, one every two metres, for a total range of 10 m. The maximal observed temperature discrepancy between two different Pt100 probes was only 0.2 K over a 10 m distance for a temperature around 297.6 K. As for the other environmental parameters, the atmospheric pressure was equal to 1001.4 hPa, the relative humidity 35.1% and the CO_2 content 500 ppm.

Part A of the acoustic system (containing the transmitter Tx 2 and receiver Rx 1) was set up close to the first temperature probe while part B (containing Tx 1 and Rx 2) was placed, successively, at five different positions. The calibration was thus performed for five different distances between the two parts of the acoustic system: 3.2 m, 4.7 m, 6.8 m, 8.9 m and 10.6 m. For each distance, 30 DTOA measurements were made and compared with a reference TOF. The latter was determined from the measured distance d and a reference speed of sound v_{ref} calculated using Cramer's equation, the local sensors of the thermometer for pressure, humidity and CO_2 content, and the Pt100 probes for the temperature:

$$t_{TOFref} = \frac{d}{v_{\mathrm{ref}}(Pt100, p, x_w, x_c)}. \tag{9}$$

Finally, the offset value was determined using a weighted least-squares fitting method (WLS). The value of the offset of the system is that which minimizes the following sum:

$$S = \sum_{j=1}^{5} w_j \times \sum_{i=1}^{30} \left[\left(t_{\mathrm{DTOA}}(i,j) - t_{TOFref}(i,j) \right) - t_{offset} \right]^2 \tag{10}$$

where i is the index of the measurements for a given distance, j is the index of the distance, and w_j the weight assigned to a series of 30 measurements. In fact, for a given series of measurements, i.e. for a distance j, all the DTOA measurements have the same weight[4]:

$$w_j = \frac{1}{\left(\sigma_{\mathrm{DTOA}} + \sigma_{TOFref}(j)\right)^2}. \tag{11}$$

The uncertainty in the measured DTOA, σ_{DTOA}, has been assessed as 1.0 µs. This value corresponds to the random noise obtained for a series of 20 successive DTOA measurements performed within two minutes in a controlled environment over a distance of about 8 m.

In addition, and as shown in formula (9), the uncertainty in the reference TOF, σ_{TOFref}, depends on the uncertainty in the measured distance, equal to 1 mm (Leica Disto d210), as well as on the uncertainty in the reference speed of sound v_{ref}. The latter is mainly due to the contribution of the temperatures measured by the Pt100 probes as shown in Table 2.

The uncertainty of each of these probes is 100 mK. The ensemble average of six sensors would be $(100/\sqrt{6})$ mK = 41 mK. However, given that measured distances varied from 1 m to 10 m while the thermometers were left in place, for the shortest paths, only two thermometers contributed. Moreover, the probe reading is that of the temperature of the sensor itself and not necessarily of the surrounding air [5]. For this reason, therefore, we have ascribed a standard uncertainty of 100 mK to all temperature calibrations, irrespective of distance.

In the end, an uncertainty of 0.06 m/s is obtained for a reference speed of sound of 343.8 m/s, i.e. 175 ppm. This result does not include the contribution of the Cramer

[4] It is not necessary to normalise the weights such that $\sum_j w_j = 1$. Thus, since the variables t_{DTOA} and t_{TOFref} are perfectly correlated, the variance is a linear and not a quadratic sum of the associated standard deviations.

Table 2. Uncertainty budget for the determination of the reference time of flight, where the distance d is measured using an absolute distance meter (ADM) and v_{ref} is calculated from the reference temperature θ, pressure p, water vapour mole fraction x_w and carbon dioxide content x_c.

Parameter	Source	Uncertainty (k=1)		Contribution to v_{ref} by Monte-Carlo	Uncertainty in the reference TOF (k=1)
d	ADM	u_d=1 mm		Not applicable	$\sigma_{TOF\,ref}$=3 µs for d=1 m
T	Pt100 probes	u_θ=0.1 K		58 mm/s	
p	Pressure sensor	u_p=1 hPa		0.04 mm/s	
x_w	Humidity sensor	u_{RH}=3%	u_{xw}= 815 ppm	44 mm/s	$\sigma_{TOF\,ref}$=6 µs for d=10 m
	Pressure sensor	u_p=1 hPa			
	Pt100 probes	u_θ=0.1 K			
x_c	CO_2 sensor	u_{xc}=80 ppm		7 mm/s	

equation which, we recall, was estimated by Gavioso [22] to be less than 200 ppm. Thus, the uncertainty on the reference TOF varies from 3 µs for a short distance of 1 m to 6 µs for a long distance of 10 m. It is therefore preferable to perform the calibration over a short distance so as to minimize the uncertainty.

Using formula (10), we obtained an offset of 197.9(1.1) µs. As is evident from Figure 6, without the weighted least-squares method, the uncertainties would have been far larger.

2.4.2 Length calibration

To determine the speed of the acoustic waves, it is necessary to know the distances over which the acoustic waves propagate. One concern is that the positions of the ADM and its target are not co-located with those of the acoustic transducers: there are two offsets, one per acoustic path, between the distance measured by the ADM (d) and those travelled by the acoustic waves (named d_1 and d_2).

First, the distances d_1 and d_2 were measured with a ruler. The offsets deduced for both were about 13 mm. They were subtracted from the distance d measured by the ADM. We estimated the error in the offsets was between −5 mm and +5 mm (uniform distribution, standard uncertainty of 1.5 mm): the error is therefore small enough that the time taken by the acoustic waves to propagate over these few millimetres is relatively constant, whatever the environmental parameters. For example, the speed of sound for a temperature of 303.15 K, a relative humidity of 50%, a pressure of 1013.25 hPa and a CO_2 content of 400 ppm is 350.60 m/s. Under these conditions, the

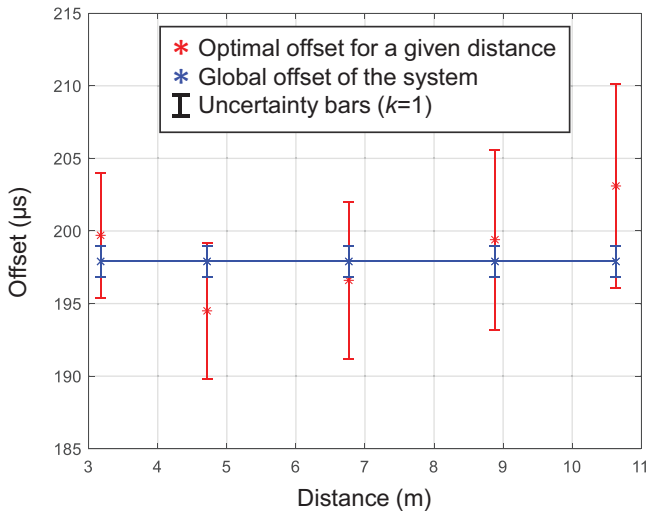

Fig. 6. Results of the calibration process for five different distances, with optimal offset for a given distance and global offset obtained by the weighted least-squares method.

acoustic waves take 4.28 µs to travel 1.5 mm. However, under the same environmental conditions, but at 283.15 K, the speed of sound is 337.47 m/s and the waves take 4.44 µs to travel 1.5 mm, i.e. 0.16 µs longer. Such a difference for a temperature variation of 20 K is equivalent to an error in the estimate of the temperature of only 28 mK at 1 m and 3 mK at 10 m.

Secondly, the errors on the offsets measured by the ruler were taken into account in the time calibration process performed at 297.6 K (in Sect. 2.4). This second correction

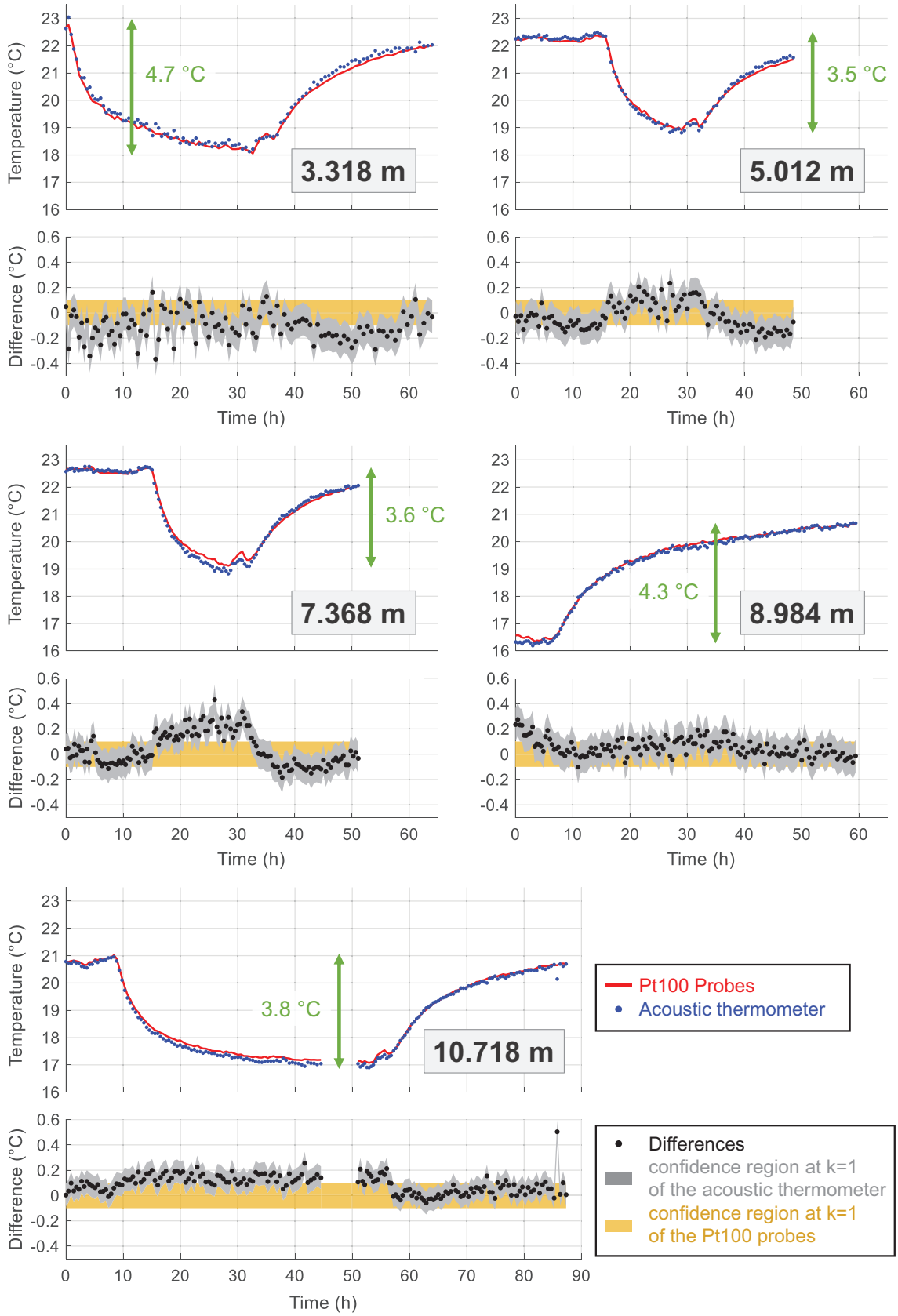

Fig. 7. Thermometry over distances from 3.3 m to 10.7 m. The gap visible for 10.718 m arose from a software glitch that caused the Matlab acquisition program to halt unexpectedly. Above: acoustic temperature (*blue* •) and reference temperature (*red* –). Below: differences (*black* •).

Table 3. Results of acoustic temperature measurements. Key: d distance; $\Delta\theta$ temperature rang u_θ temperature uncertainty.

d (m)		3.318	5.012	7.368	8.894	10.718
u_θ (K)		0.13	0.12	0.12	0.09	0.09
$\Delta\theta$ (K)		5.0	3.5	4.0	4.5	4.0
Differences	Average value (K)	-0.10	0.06	0.05	0.07	0.23
	Peak-to-valley variation (K)	0.20	0.25	0.40	0.30	0.20
	Standard deviation (K)	0.2	0.1	0.1	0.1	0.1

is valid because the systematic errors in the offsets are effectively constant whatever the environmental parameters.

Lastly, its contribution to the uncertainty of the time of flight is 0.16 µs/(2$\sqrt{3}$) = 46 ns (uniform distribution, k=1) for a 20 K temperature variation, i.e. negligible.

3 Results and discussion

3.1 Absolute temperature measurements

This section presents absolute temperature measurements made in the laboratory after calibration. The temperature is deduced from formula (5) by taking into account the instrument offset as follows:

$$v_m = \frac{d}{t_{\mathrm{D}TOA} - t_{offset}}. \tag{12}$$

As discussed previously, the uncertainties in the difference of arrival times $u(t_{\mathrm{D}TOA})$ and the offset $u(t_{offset})$ are equal to 1.0 µs and 1.1 µs, respectively. In addition, the uncertainty in the distance measured by the commercial ADM (Leica Disto d210) is equal to 1 mm. Thus, the uncertainty in the measured speed of sound v_m varies as a function of the distance and the time of flight, from 0.06 m/s at 3.2 m to 0.02 m/s at 10.6 m. From this measurement, we determine the air temperature as the value of θ for which v_m is equal to the theoretical one $v_\phi(\theta, p, x_w, x_c)$. The uncertainty in θ is around 0.13 K over 3.3 m and around 0.09 K over 10.7 m.

The acoustic thermometer was used to perform several series of measurements, for different distances from 3.3 m to 10.7 m and for temperatures ranging from 289 K to 296 K (a range limited by the air conditioning). The results are shown in Figure 7. For comparison, the Pt100 reference probes used for the previous calibration still recorded the air temperature, simultaneously with the acoustic measurements. The results of temperature measurements over the five distances are shown in Table 4.

Under the conditions of this experiment, the temperatures measured by the thermometer of uncertainty between 0.09 K and 0.13 K (k=1, and depicted by the grey area in Fig. 7) are in most cases compatible with those given by the Pt100 probes of uncertainty 0.1 K (k=1, and depicted by the yellow area in Fig. 7). However, the differences vary as a function of temperature and a pattern emerges: when the temperature falls, the value of the residuals appears to rise. This is particularly noticeable for distances of 5.012 m and 7.368 m. Thus, for low temperatures, the confidence regions can be incompatible. The linearity of the system does not appear to be very good, though it is hard to be conclusive about this since, on the one hand, the explorable temperature range is limited by the laboratory air conditioning (4.7 K max), while on the other hand, the temperature measurements are limited by their uncertainty.

3.2 Determination of Cramer coefficients

In the same way as Korpelainen and Lassila (2004) [9], we have redefined the Cramer coefficients to improve the linearity of the system. To this end, we have measured the speed of sound at 40 kHz at different temperatures. At each temperature, the speed of sound was determined from the linear regression of nine time-of-flight measurements performed at nine different distances between 1.8 m and 2.6 m. Indeed, the slope of the curve $d = f(t_{\mathrm{T}OF})$ is equal to the speed of sound. In this experiment, each time-of-flight measurement was the average of a series of 20 successive measurements, while the distance was measured with the ADM developed in-house, part of the multilateration system presented in [23]. The latter allows measurements of uncertainty of 2.5 µm (k=1). Finally, values of 341.14 m/s and 345.01 m/s were obtained for, respectively, temperatures[5] of 289.4 K and 296.3 K. The uncertainties in these values, attributed using the uncertainties in the TOF measurements and distance measurements, are equal to 0.27 m/s and 0.31 m/s.

From these two values of the speed of sound, the coefficients a_0 and a_1 of the Cramer equation presented in formula (3) were re-determined. The coefficients a_2 to a_{15} of the Cramer equation remained unchanged. The new values

[5] The choice of these values was governed by the behaviour of the air-conditioning system. It was not possible to obtain stable temperatures around 292 K or 293 K.

Table 4. Values of the coefficients a_0 and a_1 of the original Cramer equation [16] valid for zero-frequency compared with those determined by this work for 38–42 kHz and Korpelainen and Lassila for 50 kHz [9].

Coefficient	Cramer	This work	Korpelainen and Lassila
a_0 (m/s)	331.5024	331.00(1.24)	330.8860
a_1 ((m/s)/K)	0.603055	0.60(6)	0.6324

of a_0 and a_1 for sound waves at 40 kHz frequencies are 331.00 m/s and 0.60 (m/s)/K. The uncertainties in these coefficients were determined using a Monte Carlo method: data points were simulated with uncertainties in temperatures of 0.1 K and in speed of sound of about 0.3 m/s. Thus, we have obtained uncertainties of 1.24 m/s for a_0 and 0.06 (m/s)/K for a_1.

These values are too large to be usable. With only two measured values of acoustic velocity, at 289.4 K and 296.3 K, it is difficult to do any better: in future, the experiment should be repeated in a laboratory allowing greater and more carefully controlled temperature variations.

3.3 Discussion of the new values of Cramer coefficients

Table 4 shows three pairs of values of the coefficients a_0 and a_1 of the Cramer equation. The value of a_0 determined in this work lies in between that of Cramer valid for zero frequency and that of Korpelainen and Lassila measured at 50 kHz. Given that the thermophysical properties of moist air display monotonic variations with frequency, does this trend correspond to what we would expect, i.e. the speed of sound fall with frequency? If the first relaxation resonances of oxygen and nitrogen molecules are greater that 60 kHz, then the refractive index for sound, so to speak, should increase with frequency, thereby reducing acoustic velocity [20]. On the other hand, at the present level of uncertainty, the temperature-dependent coefficient a_1 is compatible with both that for 50 kHz and the zero-frequency value of Cramer. Again one would expect it to lie somewhere in between both values.

If it were possible to reduce the uncertainties, especially that of a_1, subsequent measurements at other frequencies in the range 20 kHz to e.g., 60 kHz could help shed valuable light on the dispersive properties of the Cramer coefficients that arise in practice. This is easier said than done, however. Ultrasonic transducers are designed to work in a narrow frequency range, usually a few kilohertz, so several different transducers would need to be employed. At frequencies just above 20 kHz loss of signal due to diffraction and noise from crosstalk might limit the useful accuracy. At the higher frequency end, attenuation of the ultrasonic signals ultimately becomes problematic: attenuation in air ($T = 293.15$ K, $p = 1013.25$ hPa, $RH = 50\%$) is 0.5 dB/m for an acoustic frequency of 20 kHz, rising to 1.3 dB/m at 40 kHz and 2.0 dB/m at 60 kHz.

3.4 Uncertainty in the distance measurements

3.4.1 General case

In the acoustic thermometer developed here, the average air temperature along the acoustic path is estimated by determining the temperature value for which the velocity measured by the instrument v_m is equal to that estimated by the Cramer equation $v_\phi(\theta,\ p,\ x_w,\ x_c)$. As previously explained, the uncertainty in θ is assessed around 0.13 K (k=1) over 3.2 m and around 0.09 K (k=1) over 10.7 m. The impact of acoustic thermometry for distance measurements by optical means was summarized in Table 1: for air at temperatures around 293 K, the temperature-dependence is −0.95 (µm/m)/K. A temperature uncertainty of 90 mK corresponds therefore to an uncertainty of 0.9 µm for an optical path of 10.7 m.

However, this uncertainty value of 90 mK was determined without considering the contribution of the Cramer equation which, we recall, was estimated by Gavioso [22] to be less than 200 ppm. Not taking into account this additional uncertainty allows us to show the performances that an acoustic thermometer based on low-cost components, such as the one we have developed, can reach. In the future, the first two coefficients of the Cramer equation for acoustic waves at 40 kHz, as well as an uncertainty value specific to this equation, must be estimated more accurately.

In the current state of our work, in the range from 289 K to 296 K, it has been demonstrated in Figure 7 we can measure average air temperature to better than 0.4 K for distances up to 10.7 m. Thus, the contribution of the air temperature to distance measurements by optical means will be less than 4.1 µm.

3.4.2 Presence of a temperature gradient

The acoustic thermometer developed does not measure temperature gradients along a path, but rather only an average temperature over this path. This is deduced from the average speed of sound, which could be formalized as:

$$v_m = \frac{1}{L}\int_0^L v(x)\mathrm{d}x. \tag{13}$$

where $v(x)$ is the speed of sound at the position x located on the measurement axis and L the length of this path.

If the temperature distribution (i.e. its gradient along the measured path) was known, we could deduce the distribution of the speed of sound $v(x)$ along the measured path, and so the average speed of sound v_m. However, the reverse operation is impossible.

For our application, i.e. correction of the air refractive index for dimensional measurements, the question that arises is the following: along an optical path where there would be a temperature gradient, what is the difference between the air refractive index determined from an acoustic thermometer and that determined using a hypothetical infinite number of temperature sensors along the path? In the first case, we only know the average temperature, while in the second, we have access to the temperature distribution. This question was answered in [25] using the Edlén formula: the authors assumed a temperature gradient of 0.1 K/10 mm along a measurement path of 1 m. The maximum error obtained on the calculation of the air refractive index when the temperature is measured with the acoustic thermometer was equal to about 3×10^{-8}. The induced error is therefore negligible. However, by placing several acoustic thermometers in different positions, one might be able to map the temperature inside a room and thus evaluate temperature gradients. As an example, such an approach was used at INRiM [11] to determine the vertical temperature gradient.

4 Conclusion

The present article has described the use of a time-of-flight acoustic thermometer to measure air temperature integrated along an optical path, its calibration with respect to standard platinum resistance thermometers, and an estimate of experimental uncertainty. The signal used in the system developed is a 500-μs-long pulse with a rectangular envelope shape. Among the methods investigated to detect arrival times, cross-spectrum produced the cleanest data. However, cross-correlation was the method preferred for the measurements due to its superior repeatability.

The acoustic thermometer developed yielded absolute temperature measurements in the range from 289 K to 296 K with an error less than 0.4 K for distances up to 10.7 m. However, a non-linearity of the system was identified. This problem was solved using a modified version of Cramer's equation adapted to sound waves at 40 kHz, with the same functional form as the original, but with new and more appropriate values for the coefficients a_0 and a_1 that dominate temperature dependence. The coefficients determined in our work have uncertainties too large to be usable, due to the behaviour of the air-conditioning of the laboratory in which the measurements were carried out. A natural extension of this work would be to repeat the experiment in a laboratory allowing larger and more tightly controlled climatic variations (for instance, temperature and humidity control at ±0.1 K and ±5%), and over a wider distance range, i.e., from 1 m to beyond 10 m. Measurements at other ultrasonic frequencies e.g., 20 kHz to 60 kHz, though not indispensable for the present experiment, would be a most welcome test of dispersion, especially if they were accurate enough to investigate the frequency variation of other Cramer coefficients.

In the current state of our work, for a distance of 10.7 m, the standard temperature measurement uncertainty is estimated to be 90 mK arising from time-of-flight measurements. This value does not take into account the uncertainty arising from the Cramer equation itself, which remains to be determined. While the value of 90 mK merely indicates the performance the acoustic thermometer can reach it sets a valuable lower bound on the overall temperature uncertainty to be included in refractive index calculations.

A deeper issue concerns the very validity of the semi-emplirical Cramer equation in which the physical interpretation of given terms is by no means obvious. Ultimately, a thermophysical treatment based on a microscopic approach along the lines of Zuckerwar [21] will most likely prevail and allow one to predict the parameter dependence of refractive index more accurately than any version of the Cramer equation, including the one presented here. In the meantime, the present work should allow the semi-empirical approach to continue to be useful until superseded by a truly physical model with reliably determined parameters.

This work was partially funded by Joint Research Project (JRP) 17IND03 LaVA that has received funding from the European Metrology Programme for Innovation and Research (EMPIR) co-financed by the Participating States and from the European Union's Horizon 2020 research and innovation programme. M.D. Plimmer thanks R.M. Gavioso for sharing as yet unpublished data. The authors thank C. Guianvarc'h for helpful discussions and D. Truong for expert technical assistance.

References

1. B. Edlén, The refractive index of air, Metrologia. **2**, 71–80 (1966)
2. G. Bönsch, E. Potulski, Measurement of the refractive index of air and comparison with modified Edlén's formulae, Metrologia. **35**, 133–139 (1998)
3. K.D. Froome, Precision distance measurement based on the velocity of light, Sci. Prog. **59**, 199–223 (1971)
4. P. Pérez Muñoz, J.A. Albajez García, J. Santolaria Mazo, Analysis of the initial thermal stabilization and air turbulences effects on laser tracker measurements, J. Manuf. Syst. **41**, 277–286 (2016)
5. M. de Podesta, S. Bell, R. Underwood, Air temperature sensors: dependence of radiative errors on sensor diameter in precision metrology and meteorology, Metrologia. **55**, 229–244 (2018)
6. T. Hieta, M. Merimaa, Spectroscopic measurement of air temperature, Int. J. Thermophys. **31**, 1710–1718 (2010)
7. R. Underwood, T. Gardiner, A. Finlayson, J. Few, J. Wilkinson, S. Bell, J. Merrison, J.J. Iverson, M. de Podesta, A combined non-contact acoustic thermometer and infrared hygrometer for atmospheric measurements, Meteorol. Appl. **22**, 830–835 (2015)

8. R. Underwood, T. Gardiner, A. Finlayson, S. Bell, M. de Podesta, An improved non-contact thermometer and hygrometer with rapid response, Metrologia. **54**, S9–S15 (2017)
9. V. Korpelainen, A. Lassila, Acoustic method for determination of the effective temperature and refractive index of air in accurate length interferometry, Opt. Eng. **43**, 2400–2409 (2004)
10. M. Pisani, M. Astrua, M. Zucco, An acoustic thermometer for air refractive index estimation in long distance interferometric measurements, Metrologia. **55**, 67–74 (2018)
11. M. Pisani, M. Astrua, M. Zucco. Improved acoustic thermometry for long-distance temperature measurements, Sensors. **23**, 1638 (2023)
12. $R = kN_A$ where k is Boltzmann's constant ($1.380\,649\times10^{-23}$ J/K) and N_A the Avogadro constant ($6.022\,140\,76\times10^{23}$ mol^{-1}). See the NIST fundamental constants database https://physics.nist.gov/cuu/Constants/
13. J. Lovell-Smith, An expression for the uncertainty in the water vapour enhancement factor for moist air, Metrologia. **44**, L49–L52 (2007)
14. A.H. Harvey P.H. Huang. First-Principles Calculation of the Air-Water Second Virial Coefficient, Int. J. Theromphys. **28**, 556–565 (2007)
15. G. Garberoglio, P. Jankowski, K. Szalewicz, A.H. Harvey, Fully quantum calculation of the second and third virial coefficients of water and its isotopologues from ab initio potentials, Faraday Discuss. **212**, 467–497 (2018)
16. O. Cramer, The variation of the specific heat ratio and the speed of sound in air with temperature, pressure humidity and CO _2 concentration, J. Acoust. Soc. Am. **93**, 2510–2516 (1993)
17. G.S.K. Wong, Speed of sound in standard air, J. Acoust. Soc. Am. **79**, 1359–1366 (1986)
18. G.S.K. Wong, Comments on The variation of the specific heat ratio and the speed of sound in air with temperature, pressure, humidity, and CO_2 concentration, [J. Acoust. Soc. Am. **93**, 2510–2516 (1993)], J. Acoust. Soc. Am. **97**, 3177–3179 (1995)
19. M. O'Donnell, E.T. Jaynes, J.G. Miller. General relationship between ultrasonic attenuation and dispersion, J. Acoust. Soc. Am. **63**, 1935–1937 (1978).
20. C.L. Morfey, G.P. Howell, Speed of sound in air as a function of frequency and humidity, J. Acoust. Soc. Am. **68**, 1525–1527 (1980)
21. A.J. Zuckerwar, Handbook of the speed of sound in real gases, Volume 3: Speed of Sound in Air, (Academic Press Inc., 2003)
22. R.M. Gavioso, M. Fogliati, D. Madonna Ripa, Modelling Uncertainty of Speed of Sound in Humid Air. Oral presentation. Twenty-first Symposium on Thermophysical Properties, Boulder, Colorado, USA 20–25 June 2021
23. J. Guillory, D. Truong, J.-P. Wallerand, Uncertainty assessment of a prototype of multilateration coordinate measurement system, Precis. Eng. **66**, 496–506 (2020)
24. J.C. Jackson, R. Summan, G.I. Dobie, S.M. Whiteley, S.G. Pierce, G. Hayward, Time-of-flight measurement techniques for airborne ultrasonic ranging, IEEE Trans. Ultrason. Ferroelectr. Freq. Control. **60**, 343–355 (2013)
25. M. Dobosz, M. Ciuba, Ultrasonic measurement of air temperature along the axis of a laser beam during interferometric measurement of length, Meas. Sci. Technol. **31**, 045202 (2020)

Cite this article as: Karim Mimoune, Joffray Guillory, Mark Plimmer, Acoustic thermometer operating up to 11 m: uncertainty assessment and new values for Cramer coefficients around 40 kHz, Int. J. Metrol. Qual. Eng. **14**, 13 (2023)